Int. J. Heat Mass Transfer. Vol. 36, No. 15, pp. 3823–3830, 1993
Printed in Great Britain

0017-9310/93 $6.00 + 0.00

An experimental investigation of the transient response of a water heat pipe

MOHAMED S. EL-GENK and LIANMIN HUANG
Institute for Space Nuclear Power Studies, Department of Chemical and Nuclear Engineering, The University of New Mexico, Albuquerque, NM 87131, U.S.A.

(*Received* 3 *August* 1992 *and in final form* 19 *February* 1993)

Abstract—Experiments were performed to investigate the transient response of a water heat pipe to step changes in input power at different cooling rates. The copper heat pipe employs a double-layered, 150 mesh copper screen wick and its evaporator section was uniformly heated while the condenser section was convectively cooled. The time constants of the vapor temperature and the effective power throughput, for both heat-up and cool-down transients, were determined as functions of the electric power input and the water mass flow rate in the cooling jacket of the condenser section. Both the vapor and wall temperatures were measured at ten axial locations along the heat pipe.

INTRODUCTION

UNDERSTANDING the transient operation of heat pipes is of interest to many space applications including thermal management and heat rejection radiators. Many theoretical and experimental studies of the transient operation of low temperature and high temperature heat pipes have been reported; for example refs. [1–10]. However, the focus of this study is on experimental investigations of the transient operation of water heat pipes with emphasis on obtaining data to verify an existing transient heat pipe model [4]. Although the results of several experiments of water heat pipes have been published, the measurements of the axial distribution of the vapor temperature or pressure have been inconclusive [5–8]. Schmalhofer and Faghri [5] have used multiple-point thermocouples to measure the vapor temperature at different axial locations in the vapor region; however, they obtained only one temperature measurement in the evaporator section. Consequently, the actual vapor temperature distribution in the heat pipe during the heat-up transients could not be deduced from the experimental data.

The most complete set of experimental data has been that of Fox and Thomson [6]. They measured the axial and radial vapor temperature distributions in a water heat pipe. At each of the ten axial positions in the heat pipe, the temperature was measured at four radial positions within the vapor region. However, since the transients in Fox and Thomson's experiment were initiated by changing the cooling requirements and holding the input power constant, the data is of limited use for verifying calculational models during start-up transients. Therefore, additional experimental measurements are needed of the axial distribution of the vapor temperature and/or pressure during start-up and cool-down transients.

In this work, experiments were performed which included not only measurements of the wall temperature but also the vapor temperature in the different regions of the heat pipe (evaporator, adiabatic, and condenser sections) as functions of time during heat-up and cool-down transients. The experiments investigated the response of a water heat pipe to step function changes in input power at different cooling rates of the condenser region. The evaporator section of the heat pipe was uniformly heated using an electric tape and the condenser section was convectively cooled using a water jacket. Direct measurements of the vapor and wall temperatures were obtained along the entire length of the heat pipe. The heat-up and cool-down time constants for both the effective power throughput and the vapor temperature were determined as functions of the cooling water mass flow rate and the electric power input to the heating tape of the evaporator section. The effective power throughput, P_{cool}, is determined from the heat balance in the cooling jacket of the heat pipe condenser section.

EXPERIMENTAL SETUP

As shown in Figure 1, the heat pipe was maintained in the horizontal position to minimize the gravity effect. The overhead tank in Fig. 1 was used to maintain a constant water flow rate to the condenser cooling jacket during the experiments. The water temperature was measured at the inlet and the exit of the condenser cooling jacket using K-type thermocouples, and the cooling water flow rate was measured using a rotameter. These measurements were then used to determine the effective power throughput in the heat pipe during the transient (equation (2)). The evaporator section was uniformly heated using an A.C. electric tape on the outside of the heat pipe wall (Fig. 2). The surface area of the evaporator section was 235 cm^2. The electric power input to the electric tape in

NOMENCLATURE

A	area [m^2]
C_p	specific heat [J g^{-1} K^{-1}]
D	outer diameter of insulation shell of the evaporator section [m]
g	acceleration of gravity [9.8 m s^{-2}]
h	heat transfer coefficient [W m^{-2} K^{-1}]
k	thermal conductivity [W m^{-1} K^{-1}]
$\dot{m}$	cooling water mass flow rate [g s^{-1}]
P	power [W]
Ra	Rayleigh number, $g\beta(T_s-T_a)D^3/\nu\alpha$
T	local or mean temperature [K]
t	time [s]
x	variable
X	normalized variable, $X-X_0$
z	axial position [m].

Greek symbols

α	thermal diffusivity of air [m^2 s^{-1}]
β	thermal expansion coefficient of air [K^{-1}]
ε	error in steady-state energy balance, equation (1) [W]
τ	time constant, equations (5a) and (5b) [s]
ν	kinematic viscosity of air [m^2 s^{-1}].

Subscripts

a	ambient, room
c	cool-down
cool	throughput in the heat pipe
e	electric
ex	cooling jacket exit
h	heat-up
in	inlet of cooling jacket
loss	loss by natural convection
nc	natural convection
o	initial, or beginning of a transient process
s	insulation surface
ss	steady-state
v	vapor.

the experiment was measured directly using a power meter and controlled by a resistance variac.

The heat pipe was insulated to minimize heat losses during the experiments; the ends of the evaporator and the condenser sections were also insulated. The heater of the heat pipe evaporator section was surrounded by a perlite insulation shell, which was separated from the heating tape by a small air gap (5 mm). The radial temperature distribution in the insulation was measured at two axial locations (Fig. 2). At each location, three K-type thermocouples, spaced radially as shown in Fig. 3, were used to measure the radial temperature distribution in the insulation shell. The outermost thermocouples were placed about 3 mm from the outer surface of the insulation cylinder. The perlite insulation was then wrapped in aluminum foil to minimize radiation losses. The mean surface temperature, which was based on the average value of the outermost thermocouple readings, after correcting for the temperature drop to the insulation surface (about 13 K) was used in conjunction with the room temperature to determine the heat losses by natural convection from the insulation surface in the evaporator section [11].

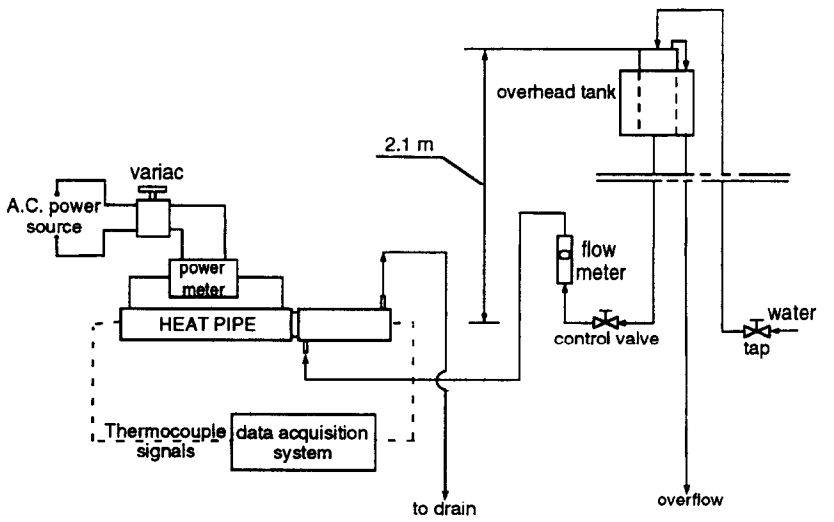

FIG. 1. A schematic diagram of the experimental setup.

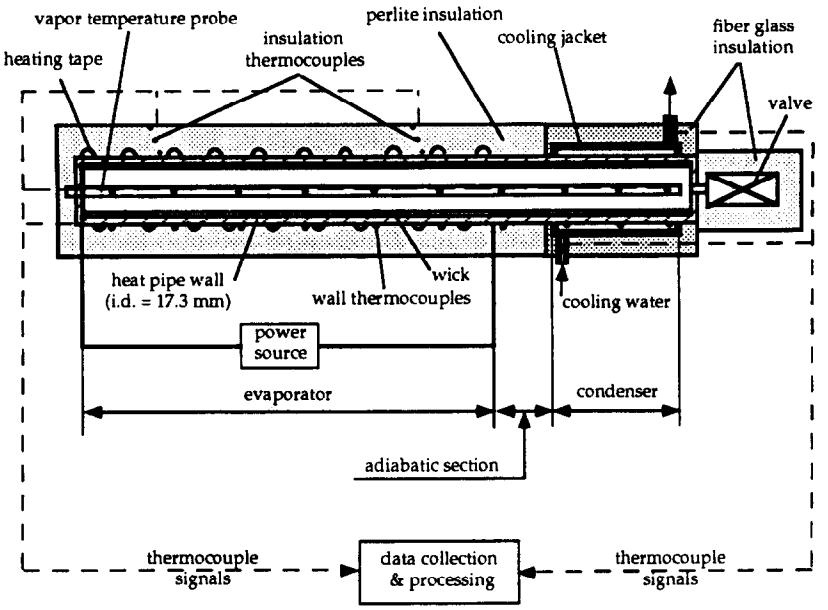

FIG. 2. A longitudinal cross-section of water heat pipe.

The water heat pipe used in the experiments consists of a copper tube (17.3 mm i.d., 19.1 mm o.d., and 610 mm long) and employs two layers of copper wick (150 mesh), a specially designed vapor temperature probe, and a condenser cooling jacket (Figs. 2 and 3). The condenser section was 170 mm long and the evaporator section was 393 mm long. In the condenser section, the heat pipe was convectively cooled using a water jacket (25.4 mm o.d. and 22.3 mm i.d.). The ball-valve at the end of the condenser allows charging

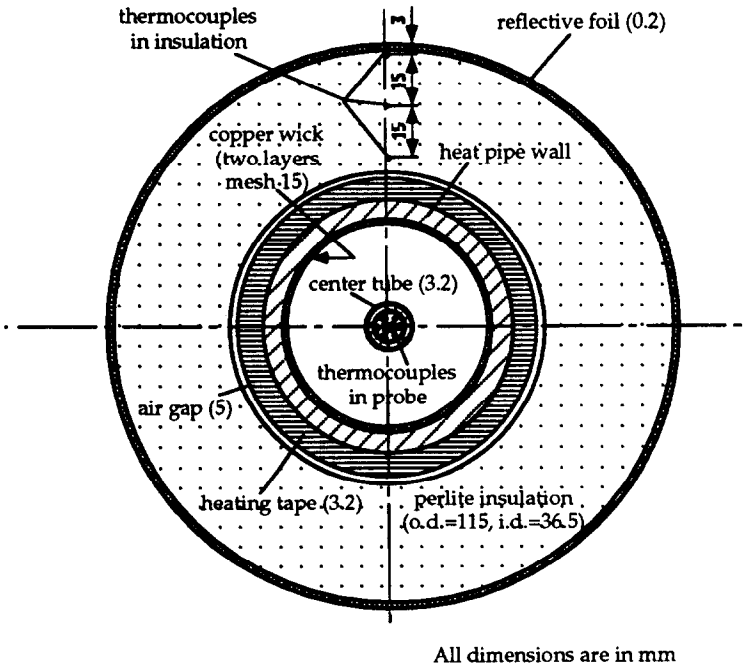

FIG. 3. Radial cross-section A–A of water heat pipe.

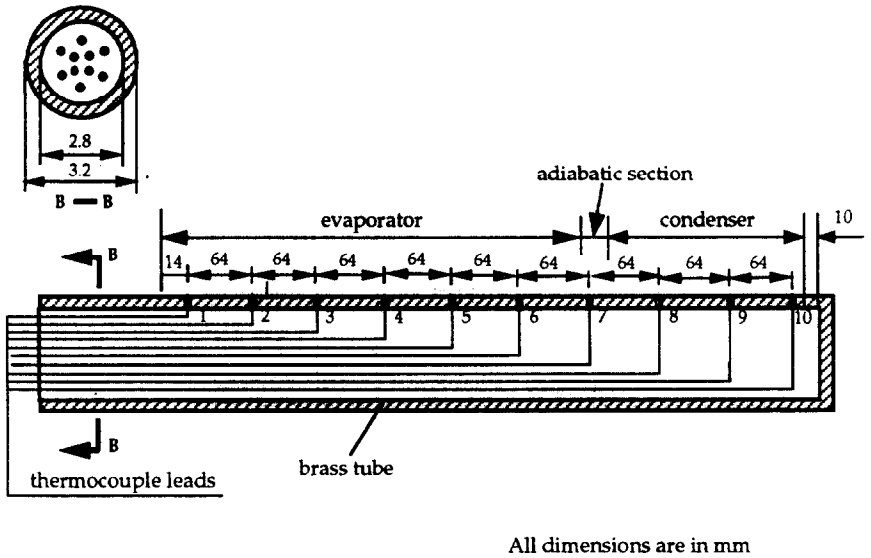

FIG. 4. A longitudinal cross-section of vapor temperature probe.

and discharging of the working fluid as well as removing the non-condensible gases from the heat pipe before performing the experiments (Fig. 2).

The vapor temperature in the heat pipe was measured at 10 axial locations using a specially designed probe instrumented with K-type thermocouples. The thermocouples were spaced in the probe as indicated in Fig. 4. The vapor temperature probe consists of a brass tube, 3.2 mm o.d. and 0.2 mm wall thickness, and 10 thermocouples. These thermocouples were inserted inside the brass tube and silver soldered to the tube wall outer surface (Fig. 4). An additional ten K-type thermocouples were used to measure the heat pipe wall temperature at the same axial locations as the vapor temperature. A total of six thermocouples were used to measure the wall temperature in the evaporator section, one thermocouple in the adiabatic section and three thermocouples in the condenser section. In order to accurately record the wall temperature, the wall thermocouples were inserted into the heat pipe wall. In the evaporator region, the wall thermocouples were also protected from the heating tape; they were covered with thermal insulation to avoid recording values higher than those of the wall, particularly since the temperature of the electric tape in the experiments could have been as high as 600 K. Similarly, the thermocouples in the condenser section were surrounded by small dry wells to physically isolate them from the water flow in the cooling jacket. A computer controlled, high speed data acquisition system was used to monitor all thermocouples measuring the temperatures of the wall, vapor, insulation, and the cooling water and to collect other experimental data.

The average temperature of the water entering the cooling jacket of the heat pipe was about 295 K, the water mass flow rate was varied from 1.9 to 14 g s^{-1}. The electric power input to the evaporator heater varied from 365 to 590 W. The accuracy of the experimental measurements was about ± 0.5 K for temperatures, about $\pm 2\%$ for electric power input, and $\pm 2\%$ for the cooling water flow rate. These measurement errors resulted in an uncertainty of about $\pm 4\%$ in determining the effective power throughput of the heat pipe and about $\pm 3\%$ in the calculated heat losses from the surface of the insulation in the evaporator section by natural convection to ambient. During the experiments, the temperatures at the insulation surface were less than 355 K, and hence radiation losses were negligible. The experimental uncertainties were calculated using the method of Kline and McClintock [12].

EXPERIMENT EXECUTION AND CALIBRATION

Before conducting the experiments, the water flow rate in the cooling jacket was stabilized at the desired value. The transient was initiated by increasing the electric power to the heating tape in the evaporator section in a step function, from zero to the required value, using the variac in the electric circuit (Fig. 1). The heat-up phase of the experiment continued until steady-state was reached. Then, the electric power to the evaporator section was reduced in a step function to zero, but the cooling water flow rate was kept unchanged. At the end of the cool-down phase of the experiment, the heat pipe and the insulation were cooled down to almost room temperature, and then another transient was initiated.

In order to verify the soundness of the experimental

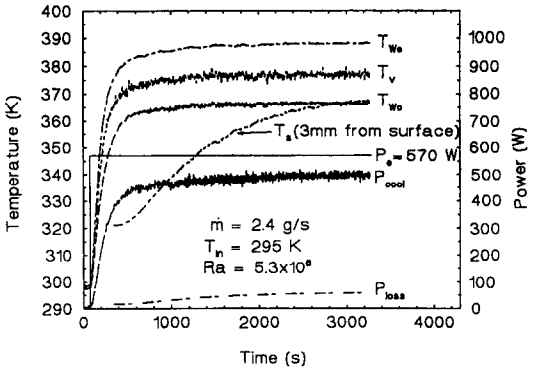

FIG. 5. Transient measurements and steady-state energy balance results.

setup, an overall, steady-state energy balance was performed. At steady-state, the energy balance in the heat pipe can be expressed as

$$P_e - P_{cool} - P_{loss} = \varepsilon \quad (1)$$

where ε is the error in the steady-state energy balance (Fig. 5). The heat losses in the condenser section of the heat pipe during the experiments were negligible because the mean water temperature in the cooling jacket was less than 320 K and the surface temperature of the insulation of the cooling jacket was almost the same as room temperature.

The effective power throughput, P_{cool}, during the transient and at steady-state was calculated from the heat balance in the cooling jacket of the condenser section as

$$P_{cool} = \dot{m}C_p(T_{ex} - T_{in}). \quad (2)$$

The heat capacity of the water is determined at its mean temperature in the cooling jacket. The steady-state heat losses by natural convection from the surface of the insulation shell in the evaporator section were determined as

$$P_{loss} = h_{nc}A_s(T_s - T_a). \quad (3)$$

The outer surface area of the insulation shell, A_s, is 0.152 m^2 and the natural convection heat transfer coefficient was determined from the following correlation [11]:

$$h_{nc} = (k/D)(0.53\,Ra^{0.25}). \quad (4)$$

The thermophysical properties of air were evaluated at the mean film temperature $((T_s + T_a)/2)$. The steady-state value of T_s varied from room temperature of 295 to 355 K. The Rayleigh number, Ra, corresponding to P_e = 580 W was about 5×10^6 (Fig. 5).

RESULTS AND DISCUSSION

This section presents the results of the steady-state energy balance in the heat pipe as well as those of the transient experiments of the water heat pipe at different electric power inputs and cooling water flow rates. The effects of these variables on the heat-up and cool-down time constants of the vapor temperature, T_v, and of the effective power throughput, P_{cool}, were investigated.

Steady-state energy balance

Figure 5 presents the results of the transient response of the water heat pipe to a step function increase in electric power input of 570 W. During the transient, the electric power and the cooling water flow rate and inlet temperature were kept constant. The heat pipe reached steady-state approximately 1500 s after the initiation of the transient. At steady-state, the sum of P_{cool} and P_{loss} was only about 11 W lower than the electric power input, for an error, ε, of about 2% (Fig. 5). This small error verified the soundness of the experimental setup and procedures.

Transient results

Figure 6 presents snapshots of the measured axial distributions of the wall and vapor temperatures at different times during the transient. The results in Fig. 6 were for the same experimental conditions as in Fig. 8. As shown in Fig. 6, the vapor temperatures were nearly uniform along the entire length of the heat pipe, with a maximum variation of about 0.9 K. Also, the measured wall temperatures in the evaporator and condenser sections were almost uniform, but different; the maximum variation in the measured wall temperatures was less than 5 K. The axial conduction in the heat pipe wall was pronounced near the end of the evaporator section, in the adiabatic section, and near the interface between the condenser and the adiabatic sections; but negligible elsewhere.

Heat-up and cool-down time constants

Two sets of experiments were performed to determine the heat-up and cool-down time constants of the heat pipe. In the first set, the electric power input was maintained constant at 575 W, while the cooling water flow rate in the condenser jacket was varied from

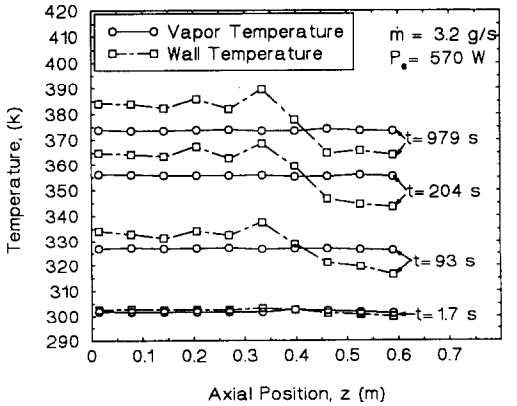

FIG. 6. Measured transient axial distributions of vapor and wall temperatures.

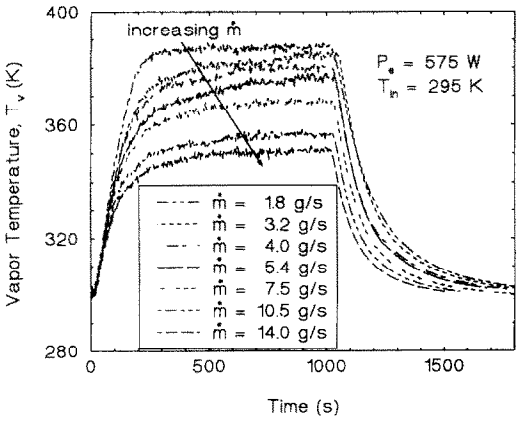

FIG. 7. Effect of cooling water flow rate on vapor temperature during heat-up and cool-down transients.

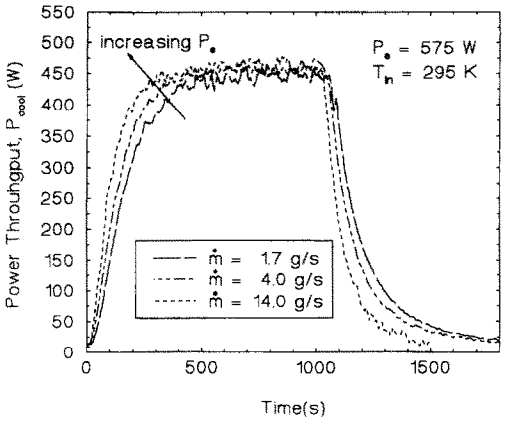

FIG. 10. Effect of cooling water flow rate on effective power throughput, P_{cool}, during heat-up and cool-down transients.

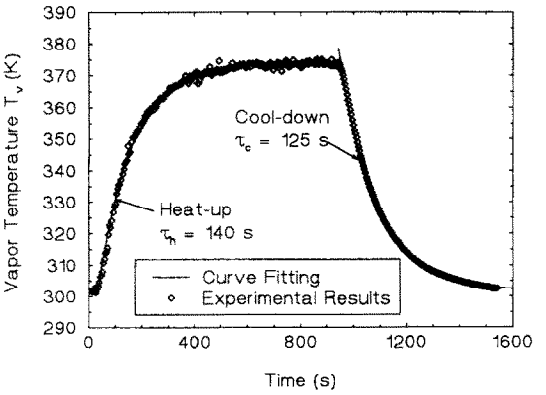

FIG. 8. Determination of vapor temperature time constants during heat-up and cool-down transients.

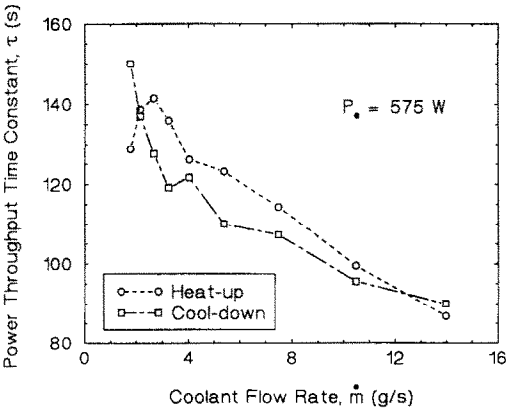

FIG. 11. Effective power throughput time constants as functions of cooling water flow rate.

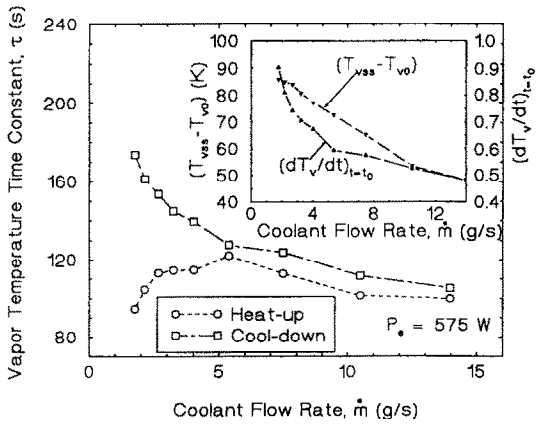

FIG. 9. Vapor temperature time constants as functions of cooling water flow rate.

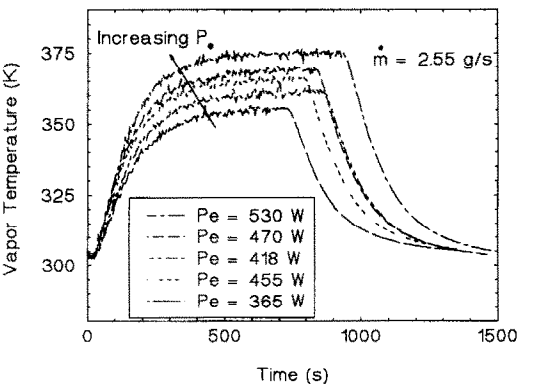

FIG. 12. Effect of electric power input on vapor temperature during heat-up and cool-down transients.

1.77 to 14 g s^{-1} (Figs. 7–11). In the second set of experiments, the cooling water flow rate was held constant at 2.55 g s^{-1}, while the electric power input to the evaporator section was varied from 365 to 580 W (Figs. 12–15). In all experiments, when steady-state was reached, the electric power to the evaporator section was reduced to zero in a step function, while the cooling water flow remained unchanged.

To determine the heat-up and cool-down time constants for a given variable, X, the experimental

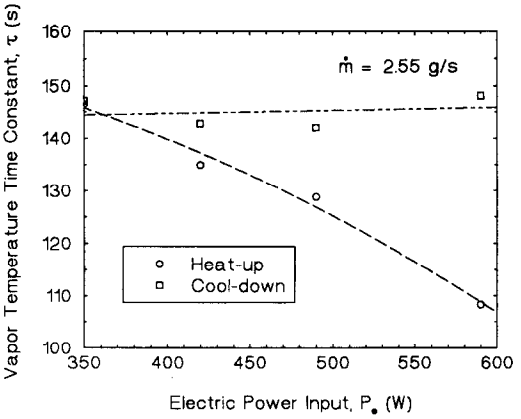

FIG. 13. Effect of electric power input on vapor temperature time constants.

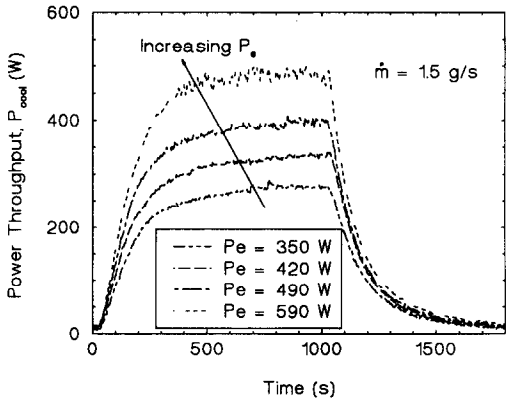

FIG. 14. Effect of electric power input on effective power throughput, P_{cool}, during heat-up and cool-down transients.

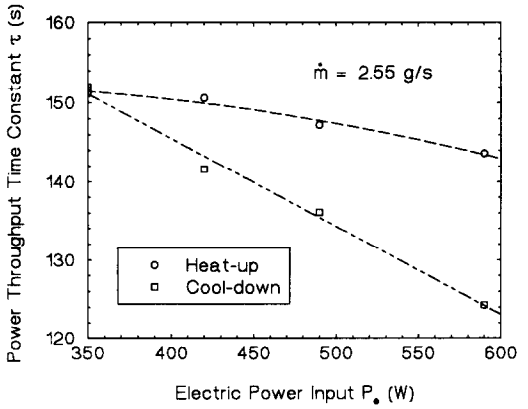

FIG. 15. Effect of electric power input on the effective power throughput time constant.

data for that variable (e.g. T_v or P_{cool}) was curve fitted using the following exponential relations:

$$X(t) = X_{ss}(1 - e^{-(t-t_0)/\tau_h}), \quad \text{during heat-up} \quad (5a)$$

and

$$X(t) = X_{ss}\, e^{-(t-t_0)/\tau_c}, \quad \text{during cool-down.} \quad (5b)$$

Figure 8 shows how the vapor temperature transient data was used, in conjunction with equations 5(a) and 5(b), to determine the heat-up and cool-down time constants. The vapor temperatures shown in Figs. 7 and 8 are the average readings of the thermocouples in the vapor temperature probe along the heat pipe. As indicated earlier, the maximum variation between these thermocouple readings was less than 1 K. In Fig. 8, the vapor temperature heat-up time constant (140 s) was slightly higher than that for the cool-down process (125 s).

In equations (5a) and (5b), the heat-up time constant can be expressed as the ratio of the steady-state values of X divided by the slope at the beginning of the transient as

$$\tau_h = |X_{ss}/[(dX/dt)_{t=t_0}]|. \quad (6)$$

This equation indicates that the time constant for either the heat-up or the cool-down transient depends not only on the steady-state value of the variable of interest (e.g. T_v or P_{cool}), but also on its rate of change at the beginning of the transient, which is confirmed by the experimental results in Figs. 9 and 11.

Effect of cooling water flow rate on time constants

Both the steady-state value of the vapor temperature and its rate of change at the beginning of the heat-up transient decreased as the cooling water mass flow rate was increased (Figs. 7 and 9). However, at flow rates below 5 g s^{-1}, the former decreased slower than the latter, causing the heat-up time constant to initially increase, reaching a maximum value of approximately 120 s, at a flow rate of approximately 5.5. g s^{-1}. Beyond this point, the vapor temperature heat-up time constant decreased as the mass flow rate was increased. For the cool-down transient the time constant decreased monotonically with the mass flow rate.

Figure 10 presents the experimental results delineating the effect of increasing the cooling water flow rate on the heat-up and cool-down transients of the heat pipe. These results were for an electric power input of 575 W and inlet water temperature to the condenser cooling jacket of 295 K. The comparison of the transient results in Figs. 7 and 10 indicate that while increasing the water flow rate caused the steady-state values of the vapor temperature to decrease appreciably, it only slightly affected the steady-state value of P_{cool}. The effect of the cooling water flow rate on the time constants of P_{cool} was similar to that for T_v. However, the heat-up time constant for P_{cool} was higher than that for T_v at low cooling water flow rate, but decreased as the water flow rate was increased. Conversely, the cool-down time constant for P_{cool} was lower than that for T_v at low water flow rates and decreased as the mass flow rate was increased (Figs. 9 and 11).

Effect of electric power input on time constants

The results of the second set of transient experiments are presented in Figs. 12–15. As indicated earlier, in these experiments, the cooling water flow rate of 2.55 g s^{-1} was the same in all experiments, but P_e was varied from 365 to 590 W. Increasing the electric power input increased the steady-state values of T_v and P_{cool}, but caused their heat-up time constants to decrease (Figs. 12–15). The cool-down time constant of T_v ($\simeq 145$ s) was almost independent of the electric power input, while that of P_{cool} decreased as P_e was increased (Figs. 13 and 15).

The effect of the electric power input on the steady-state values and the time constants of P_{cool} is shown in Figs. 14 and 15. As the results in these figures indicate, increasing P_e increased the steady-state values of P_{cool}, but caused its heat-up and cool-down time constants to decrease. A comparison of the results in Figs. 13 and 15 shows that the heat-up time constants for T_v were lower than those for P_{cool} and decreased faster as the electric power input was increased.

SUMMARY AND CONCLUSIONS

Transient experiments were performed using a water heat pipe having a uniformly heated evaporator section and a convectively cooled condenser section. Transient response of the heat pipe to step changes of the input electric power to the evaporator heater, at different cooling rates, was investigated. The heat pipe has a 393 mm long evaporator section, 37 mm long adiabatic section, and 170 mm long condenser section and employs a double-layered, 150 mesh copper wick. The time constants for the vapor temperature and the effective power throughput during the heat-up and cool-down transients were determined as functions of the electric power input and the cooling water mass flow rate.

The axial distribution of the vapor temperature was measured using a specially designed probe, which was installed along the center line of the heat pipe. The axial distribution of the wall temperature was also measured. In the transient experiments, the vapor temperature was uniform along the heat pipe. Also, the wall temperature in the evaporator and the condenser sections was almost uniform (maximum variation less than 5 K), except near the interfaces with the adiabatic section, where axial conduction in the wall was most pronounced.

Results showed that the response of the heat pipe, during the heat-up and cool-down transients can be described by an exponential function (equation (5)). The time constants for the vapor temperature and the effective power throughput depend on their steady-state values and their rates of change at the beginning of the transient (equation (6)). Increasing the electric power input or decreasing the cooling water flow rate increased the steady-state value of the vapor temperature. Also, the heat-up time constants of the vapor temperature and of the effective power throughput increased initially, then decreased as either the electric power input or the cooling water flow rate was increased. The cool-down time constant of the vapor temperature was almost independent of the electric power input, but decreased as the cooling water flow rate was increased. By constrast, both the heat-up and cool-down time constants of P_{cool} decreased as the electric power input was increased.

Acknowledgements—This research is funded under NASA Grant No. NAG3-941 to the University of New Mexico's Institute for Space Nuclear Power Studies.

REFERENCES

1. W. S. Chang and G. T. Colwell, Mathematical modeling of the transient operating characteristics of a low-temperature heat pipe, *J. Numer. Heat Transfer* **8**, 169–186 (1985).
2. A. Fahgri, Vapor flow analysis in a double-walled concentric heat pipe, *J. Numer. Heat Transfer* **10**, 583–595 (1986).
3. J. T. Seo and M. S. El-Genk, A transient model for liquid metal heat pipes, *Space Nuclear Power Systems 1988*, CONF-88000, Orbit Book Co. Inc., Malabar, FL, 9, 404–417 (1990).
4. J.-M. Tournier and M. S. El-Genk, "HPTAM" heat pipe transient analysis model: an analysis of water heat pipes, *Proc. 9th Symp. Space Nuclear Pwr Syst. Am. Inst. Physics Conf. Proc. No. 246*, Vol. 3, pp. 1023–1037 (1992).
5. J. Schmalhofer and A. Faghri, A study of circumferentially heated and block-heated heat pipes Part I: experimental analysis and generalized analytical prediction of capillary limits, *ASME Annual Winter Meeting*, Atlanta, Georgia, 2–5 December (1991).
6. R. D. Fox and W. J. Thomson, Internal measurements of a water heat pipe, *Proc. Intersociety Energy Conversion Engineering Conference*, Las Vegas, Nevada, Paper No. IECEC-709106, Vol. 7, pp. 2–76, 21–25 September (1970).
7. N. J. Gernert, Analysis and performance evaluation of heat pipes with multiple heat source, *Proc. AIAA/ASME 4th Joint Thermophysics Heat Transfer Conf.*, Boston, MA, 2–4 June (1986).
8. J. Bowman *et al.*, Transient heat pipe modeling, paper 2, *Proc. 28th Aerospace Science Meeting*, Reno, Nevada, Paper No. AIAA-90-0061, pp. 1–7, 8–11 January (1990).
9. M. S. El-Genk and J. T. Seo, A study of the SP-100 radiator heat pipes response to external thermal exposure, *J. Propulsion Pwr* **6**(1), 69–77 (1990).
10. F. Issacci, I. Catton and N. M. Ghoniem, Vapor dynamics of heat pipe start-up, *J. Heat Transfer* **113**, 985–994 (1991).
11. B. V. Karlekar and R. M. Desmond, *Engineering Heat Transfer*, p. 444. West Publishing Company, NY (1977).
12. M. Kline and F. A. McClintock, Describing uncertainties in single-sample experiments, *Mech. Engng*, 3–8 January (1953).